Synthesis and Photoinduced Electron Transfer Processes of Rotaxanes Bearing [60]Fullerene and Zinc Porphyrin: Effects of Interlocked Structure and Length of Axle with Porphyrins

Atula S. D. Sandanayaka,[†] Nobuhiro Watanabe,[‡] Kei-Ichiro Ikeshita,[§] Yasuyuki Araki,[†] Nobuhiro Kihara,[§] Yoshio Furusho,[§,||] Osamu Ito,*[,†] and Toshikazu Takata*[,‡]

Institute of Multidisciplinary Research for Advanced Materials, CREST (JST), Tohoku University, Katahira 2-1-1, Aoba-ku, Sendai 980-8577, Japan, Department of Organic and Polymeric Materials, Tokyo Institute of Technology, Ookayama, Meguro, Tokyo 152-8552, Japan, and Department of Applied Chemistry, Graduate School of Engineering, Osaka Prefecture University, 1-1 Gakuen-cho, Sakai-shi, Osaka 599-8531, Japan

Received: September 15, 2004; In Final Form: November 23, 2004

Three rotaxanes, with axles with two zinc porphyrins (ZnPs) at both ends penetrating into a necklace pending a C_{60} moiety, were synthesized with varying interlocked structures and axle lengths. The intra-rotaxane photoinduced electron transfer processes between the spatially positioned C_{60} and ZnP in rotaxanes were investigated. Charge-separated (CS) states $(ZnP^{\bullet+}, C_{60}^{\bullet-})_{rotaxane}$ are formed via the excited singlet state of ZnP (^{1}ZnP*) to the C_{60} moiety in solvents such as benzonitrile, THF, and toluene. The rate constants and quantum yields of charge separation via ^{1}ZnP* decrease with axle length, but they are insensitive to solvent polarity. When the axle becomes long, charge separation takes place via the excited triplet state of ZnP (^{3}ZnP*). The lifetime of the CS state increases with axle length from 180 to 650 ns at room temperature. The small activation energies of charge recombination were evaluated by temperature dependence of electron-transfer rate constants, probably reflecting through-space electron transfer in the rotaxane structures.

Introduction

One of the most striking features of interlocked molecules such as catenanes and rotaxanes[1] is that the constituting components are located spatially within a certain distance without any strong linkage such as covalent bonds. Therefore, the components have a high freedom of mobility. Although sophisticated supramolecular systems with specific functions characteristic of mechanical bonding or intercomponent interaction have attracted much attention, the synthesis of such molecules has always been fraught with difficulty in functionalization without damage to the interlocked structures. Much effort has hitherto been paid to the development of construction methods of interlocked structures to facilitate the syntheses of groups of interlocked molecules.[2] However, both the development of synthetic methods and the synthesis of novel functionalized interlocked molecules are significant subjects in a variety of research fields, where interlocked molecules or structures can play key roles. In addition to developing new synthetic methods for interlocked molecules,[3] we have studied the syntheses of functionalized interlocked molecules designed for asymmetric catalysis,[4] photoinduced electron transfer,[5] and so on.

Photoinduced electron transfer processes of zinc porphyrin (ZnP)−fullerene (C_{60} or C_{70}) and zinc phthalocyanin (ZnPc)−fullerene systems have gained great attention in relation to photovoltaic cells and photonic devices in the last decade.[6−8] In these systems, ZnP (or ZnPc) and C_{60} (or C_{70}) act as photosensitizers depending on the excitation wavelength; ZnP (or ZnPc) acts as an electron donor while C_{60} (or C_{70}) acts as an electron acceptor in their ground and excited states. In polar solvents, intermolecular electron transfer takes place mainly via the excited triplet states of ZnPc and/or C_{60} (or C_{70}) under appropriate concentrations.[9−11] Although electron transfers via excited singlet states are possible when concentrations of ZnP (or ZnPc) and C_{60} (or C_{70}) are high enough to compete with the intersystem crossing of the photoexcited singlet states,[12] it is actually difficult to achieve such high concentrations for ZnP (or ZnPc) and C_{60} (or C_{70}). For ZnP (or ZnPc) and C_{60} (or C_{70}) systems, intermolecular electron transfer occurs within the diffusion-controlled limit; thus, apparent electron-transfer rates are 10^7 s^{-1} under concentrations of ca. 10 mM in polar solvents.[9] Second-order back electron transfer, which is a proof of encounter between the freely solvated radical cation and the radical anion in polar solvents, also occurs within the diffusion-controlled limit; since radical ion concentration is usually as low as 10^{-6} M by single laser pulse irradiation, the radical ions usually persist for longer than 100 μs.[9]

In the case of covalently bonded ZnP and C_{60} dyads, intramolecular charge separation mainly takes place through bonds via the excited singlet states of the components depending on the excitation wavelength.[12−17] The rate constants for such charge-separation processes via singlet excited states are larger than 10^9 s^{-1} and depend on the length of the covalently bonded space and the spatial distance between ZnP and C_{60}. In several cases, charge separation via the excited triplet state takes place on the order of 10^7 s^{-1}.[18] In these dyad systems, long-lived charge-separated states as well as fast back electron transfers

* Authors to whom correspondence should be addressed. E-mail: ito@tagen.tohoku.ac.jp; ttakata@polymer.titech.ac.jp.
[†] Tohoku University.
[‡] Tokyo Institute of Technology.
[§] Osaka Prefecture University.
[||] Present address: Yashima Super-Structured Helix Project, JST, Moriyama-ku, Nagoya 552-8555, Japan.

10.1021/jp045831w CCC: $30.25
Published on Web 01/19/2005

were observed.[18] Multistep charge-transfer systems have also been investigated.[19−22]

Coordinated supramolecular ZnP (or ZnPc) and C_{60} derivatives with appending pyridine and imidazole groups, which are capable of coordinating to the Zn atom, have also been studied, revealing that charge separation via the excited singlet states in a rate of 10^9 s^{-1} takes place in intermediary polar solvents;[23,24] however, long-lived charge-separated states have been difficult to achieve, because of the restricted use of polar solvents which destroy the coordinated supramolecular systems. For multi-interaction systems with both hydrogen and coordination bonds, relatively longer-lived charge-separated states have been reported.[25]

A photoinduced electron transfer process in rotaxane in which no direct covalent bonds are present to place electron donor and acceptor has been reported.[26−28] In rotaxane systems containing ZnP (or ZnPc) and C_{60} derivatives, the charge-separation process has been reported to take place via the excited singlet states of ZnP (or ZnPc), producing a relatively long-lived charge-separated state.[5,26] These electron-transfer processes are expected to occur through space.[5] Through-space electron-transfer processes within a definite distance are important in relation to biological electron-transfer systems, including photosynthetic systems.[29] In the present study, we synthesized three rotaxanes containing spatially positioned ZnP and C_{60} moieties, as shown in Figure 1, in which the axle structure and length were changed to reveal the effect of the mobility and distance of the ZnP and C_{60} moieties on the charge-separation routes; it was found that the charge-separation route changed from the excited singlet state route to the triplet state route with axle length change. It was also revealed that the solvent and temperature also affect the route and efficiency of the electron transfer.

Results and Discussion

Syntheses of Rotaxanes. Rotaxanes **1a**−**c** with an appended fullerene on the necklace wheel and two zinc porphyrins at both ends of the axle were synthesized according to Scheme 1, where **a**−**c** correspond to three types of spacers. The construction of the rotaxane structures was carried out by the "threading approach" using hydrogen bonding interactions of secondary amide groups.[30] We previously reported that macrocycle **4** is a fine precursor for the construction of interlocked compounds.[31] Two secondary amide groups in **4** provide hydrogen bonding sites to induce an interlocked structure, whereas the sulfolene group acts as a masked diene moiety providing a 1,3-diene via the elimination of SO_2 upon heating.[32] The synthesis of rotaxane **7** was achieved by condensation of diacid choloride **5** and 5,10,15-tris(3,5-di-*tert*-butylphenyl)-20-(4-aminophenyl)porphyrin (**6**)[33] in the presence of **4** in $CHCl_3$ at 0 °C. The porphyrin moieties were used not only for effective electron donors but also for stoppers to prevent the wheel from slipping out from the axle. The yields of **7a** and **7b** were 17% and 9%, respectively, which are comparable to those of other related secondary-amide-based rotaxanes; meanwhile, **7c** was obtained in good yield (51%), indicating that **5c** is a very effective diacid chloride with which to prepare interlocked compounds.[34] The C_{60} moiety was introduced into the rotaxane by a Diels−Alder reaction. Thus, refluxing **7** with 5 equiv of C_{60} in dichlorobenzene afforded rotaxane **8** in 69−74% yield. Free porphyrin moieties **7** and **8** were converted into zinc porphyrin complexes **2** and **1**, respectively.

The structures of the rotaxanes were unambiguously characterized by NMR, MS, and elemental analyses. Figure 2 shows

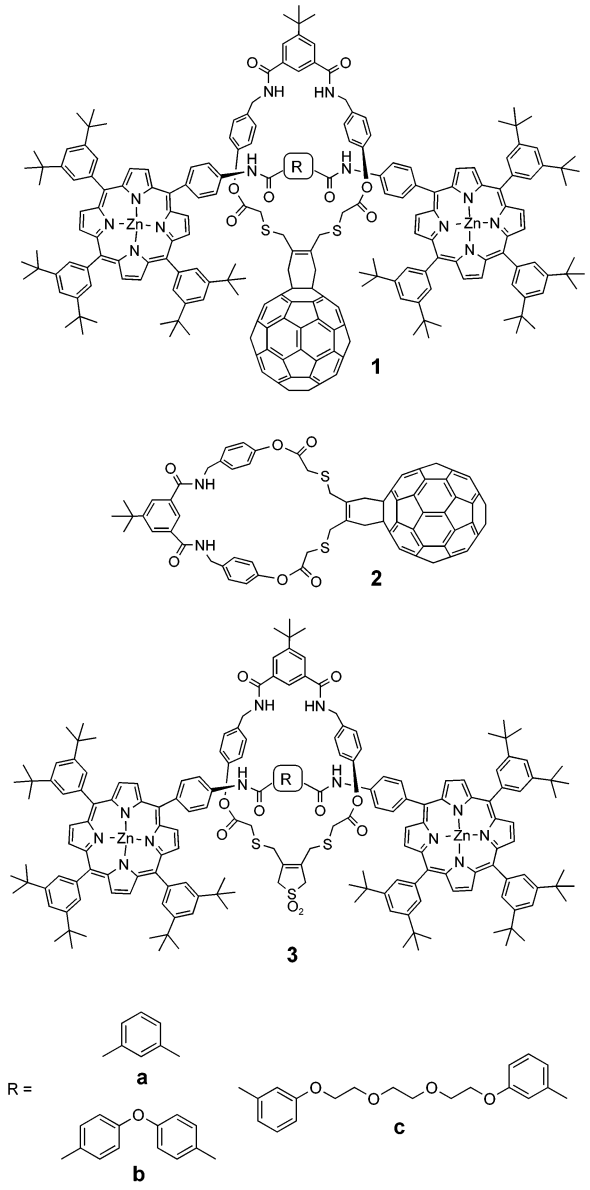

Figure 1. Molecular structures of **1a**−**c** and reference molecules.

the ^{1}H NMR spectra of wheel **4**, rotaxane **3a**, and fullerene-containing rotaxane **1a**. The spectrum of **3a** clearly consists of a superimposition of both wheel **4** and axle components in a 1:1 integral ratio (Figure 2b). Amide protons of the axle of **3a** show a remarkable downfield shift (from 6.3 to 8.0 ppm) that provides reliable evidence for intramolecular hydrogen bonding working between the wheel and the axle.[35] Some of the signals of the wheel shifted upfield due to the ring current effect of the aromatic groups in the axle component. The ^{1}H NMR spectra of **3b** and **3c** have similar features to those of **3a**. As shown in Figure 2c, the introduction of fullerene into the rotaxane has the effect of broadening the ^{1}H NMR spectrum. The spectral broadening is probably caused by the slow conformational inversion of the six-membered ring on the NMR time scale as observed for related Diels−Alder adducts of fullerene.[36] Similarly broad spectra were also observed for **1b** and **1c**. Figure 3 shows the ^{13}C NMR spectrum of rotaxane **1c**. Sixteen sp^2 carbon signals and one sp^3 carbon signal, which are characteristic of a symmetrically 1,2-substituted fullerene moiety, were clearly observed in the aromatic region and at 62.5 ppm, respectively.[37]

Molecular Structure Calculations. Molecular structures were optimized by the MM3 force field obtained from the

SCHEME 1: Synthetic Route of Rotaxanes

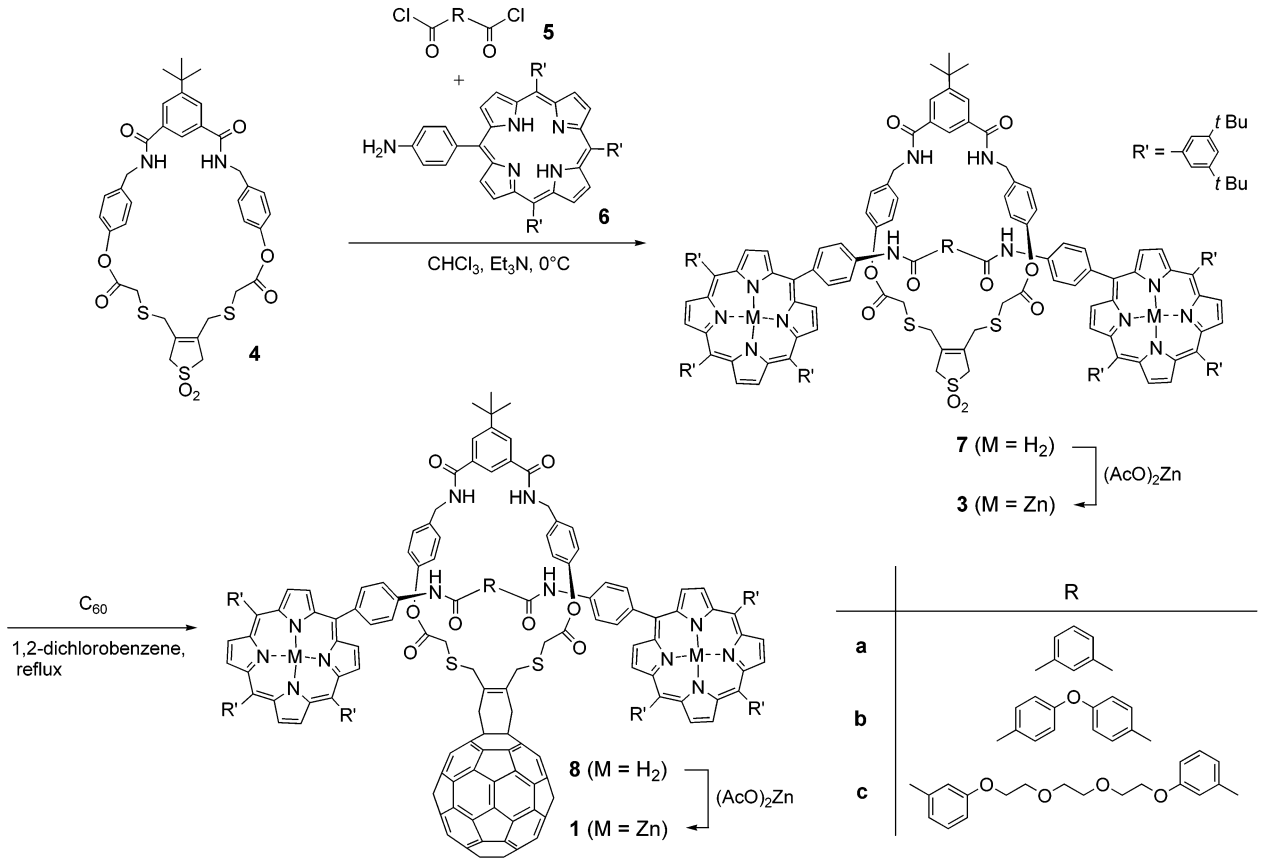

MacroModel package.[38] Although the calculated structure fluctuated at room temperature (300 K),[5b,14c] as shown in Figure 4A for **1a**, one of the ZnP moieties approached the C_{60} moiety. The center-to-center distances (R_{CC}) were evaluated from the maximal probable values, as shown in Figure 4B for **1a**, **1b**, and **1c** to be 7.0, 7.5, and 8.1 Å, respectively. The widths of fluctuation of the R_{CC} values were about 0.5 Å.

Typical structures at room temperature with the most probable R_{CC} values are shown in Figure 5. In **1a** and **1c**, a distant ZnP moiety does not have a tendency to approach the C_{60} moiety, while in **1b** a distant ZnP moiety does have that tendency. These fluctuations in molecular structure, which dynamically change the R_{CC} values, are one of the characteristics of [2]rotaxane.

Electrochemistry. From cyclic voltammetry measurements, the E_{ox} and E_{red} values were evaluated to be $E_{ox} = 0.29$ V and $E_{red} = -1.10$ V for **1a**, $E_{ox} = 0.26$ V and $E_{red} = -1.06$ V for **1b**, and $E_{ox} = 0.28$ V and $E_{red} = -1.08$ V for **1c** vs ferrocene/ferrocenium (Fc/Fc^+) in PhCN (Supporting Information, Figure S1). The E_{ox} values were attributed to those of the ZnP moieties, while the E_{red} values were assigned to those of the C_{60} moieties. In the three rotaxanes, almost the same E_{ox} and E_{red} values were observed. The free-energy changes (ΔG_{RIP}) of the radical ion pair $(ZnP^{\bullet+},C_{60}^{\bullet-})_{rotaxane}$, charge separation ($\Delta G_{CS}$), and charge recombination (ΔG_{CR}) were calculated by eqs 1 and 2, as listed in Table 1, where $\Delta G_{RIP} = \Delta G_{CR}$.[39]

$$\Delta G_{RIP} = -\Delta G^{S}_{CR} = -E_{ox} + E_{red} - \Delta G_{S} \quad (1)$$

$$-\Delta G_{CS} = \Delta E_{0-0} - \Delta G_{RIP} \quad (2)$$

In eqs 1 and 2, ΔE_{0-0} and ΔG_S refer to the energies of the lowest excited state of ZnP and the solvation of $(ZnP^{\bullet+},C_{60}^{\bullet-})_{rotaxane}$, respectively, in which solvation energy was calculated by the equation in the footnote of Table 1. The ΔG_{CS} values via ^{1}ZnP* (ΔG^{S}_{CS}) and ^{3}ZnP* (ΔG^{T}_{CS}) are all negative, predicting that both CS processes are possible for **1a**−**c** in polar and nonpolar solvents, although the ΔG^{S}_{CS} values are more negative than the ΔG^{T}_{CS} values, which are only slightly negative.

Steady-State Absorption and Fluorescence Studies. Figure 6 shows the steady-state absorption spectra of **1b** in PhCN. The absorption bands at 420 and 500−600 nm are mainly attributed to the Soret and Q-bands of the ZnP moiety, respectively. The absorption bands of the C_{60} moiety appeared at 700 nm and below 350 nm. Although the absorption spectrum of **1b** is almost a superposition of those of references **2** and **3b**, new weak bands in the 750−800 nm region were observed, indicating that there is a weak charge-transfer (CT) interaction in the ground state. Similar absorption spectra were obtained for **1b** in toluene and THF. For **1a** and **1c**, similar weak CT bands were also observed. By laser light excitation at 532 nm, ZnP was selectively excited.

The steady-state fluorescence spectrum of **1b** in PhCN observed with excitation at 532 nm is shown in the inset of Figure 6. The fluorescence peaks at 620 and 670 nm are attributed to the ZnP moiety, while the fluorescence peak of C_{60}, which is expected to appear at 725 nm, may be hidden in the fluorescence bands of the ZnP moieties. The fluorescence intensity of **1a** and **1b** was quite weak compared to those of references **3a** and **3b** in PhCN, THF, and toluene. Furthermore, enhancement of the fluorescence of the C_{60} moiety at 725 nm was not observed, suggesting that energy transfer from the ZnP moiety (^{1}ZnP*) in the excited singlet state to the C_{60} moiety may not take place. These observations indicate that electron transfer occurs predominantly from the ^{1}ZnP* moiety to the C_{60} moiety. In the case of **1c**, no appreciable decrease in

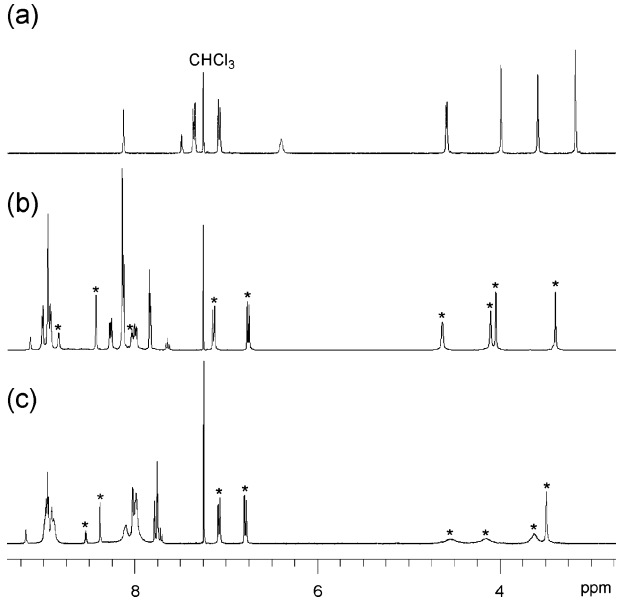

Figure 2. Partial ^{1}H NMR spectra (400 MHz, in $CDCl_3$, 328 K) of (a) macrocycle **4**, (b) rotaxane **3a**, and (c) rotaxane **1a**. The peaks denoted by an asterisk correspond to the protons of the macrocycle.

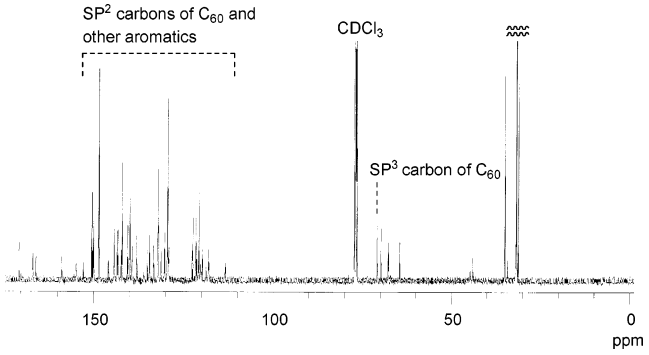

Figure 3. ^{13}C NMR spectrum of rotaxane **1c** (100 MHz, $CDCl_3$, 323 K).

fluorescence intensity was observed in relation to that of reference **3c**.

Fluorescence Lifetime Measurements. The fluorescence lifetimes (τ_f) of **1a**, **1b**, and **1c** and of the references were measured by a time-correlated single-photon-counting apparatus with excitation at 410 nm. Figure 7 shows the time profiles of the fluorescence at 625 nm of the ZnP moieties in rotaxane **1b**, which exhibits single-exponential decay in PhCN, THF, and toluene. The τ_f values of the ZnP moieties in rotaxane **1b** are shorter than that of reference sample **3b**. The τ_f values of the ZnP moieties in **1c** evaluated by the single-exponential curve-fitting method are summarized in Table 2. These τ_f values are short relative to that of the references (τ_{f0}) in both polar and nonpolar solvents. In **1a**, a rather fast fluorescence single-exponential decay was observed in PhCN, while in THF and toluene biexponential decay was observed; the τ_f values evaluated by the curve-fitting method are short relative to the τ_{f0} value, while slower parts are almost the same as τ_{f0}. To explain the appearance of the slow decay part, exciplex formation can be considered, in addition to the delayed fluorescence mechanism.[40] The τ_f values become longer with increasing donor−acceptor distance (Table 1). The τ_f values of rotaxanes **1a**, **1b**, and **1c** suggest that charge separation occurs from ^{1}ZnP* in toluene. From these τ_f values, the rate constant (k^S_{CS}) and quantum yield (Φ^S_{CS}) for charge separation via the

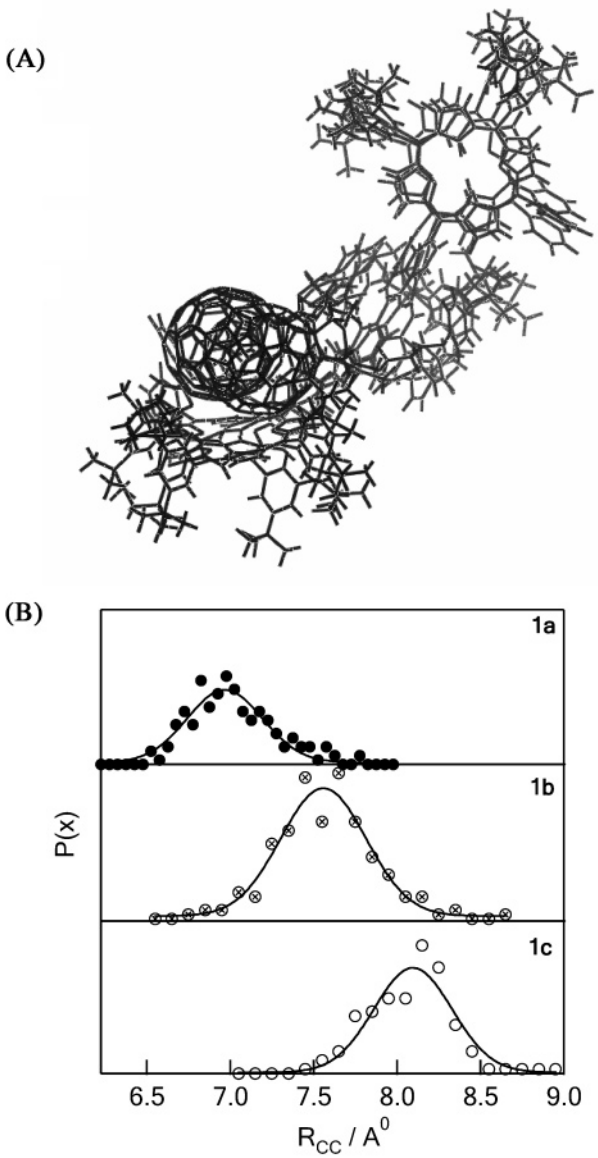

Figure 4. (A) Molecular dynamic simulations of **1a** obtained by MacroModel and (B) probability of distribution $P(x)$ vs R_{CC} of rotaxanes **1a**, **1b**, and **1c**.

^{1}ZnP* moiety were calculated by the following equations (3 and 4) as listed in Table 2.[28]

$$k^S_{CS} = (1/\tau_f) - (1/\tau_{f0}) \quad (3)$$

$$\Phi^S_{CS} = [(1/\tau_f) - (1/\tau_{f0})]/(1/\tau_f) \quad (4)$$

With axle length and R_{CC}, both k^S_{CS} and Φ^S_{CS} tend to decrease from **1a** to **1c**. For **1b** and **1c**, both k^S_{CS} and Φ^S_{CS} values in polar solvents (PhCN and THF) are larger than those in nonpolar solvent (toluene). For **1a**, both k^S_{CS} and Φ^S_{CS} values in PhCN are large, while in THF these values are slightly smaller than those in toluene.

Time-Resolved Transient Absorption Spectra. Time-resolved transient absorption spectra of **1a**, **1b**, and **1c** in PhCN, THF, and toluene were measured by nanosecond laser photolysis with 532 nm laser excitation (6 ns laser pulse). Figure 8 shows the nanosecond transient absorption spectra of **1b** in PhCN. The transient absorption band at 1000 nm observed immediately after the laser pulse (6 ns) was assigned to the anion radical of the

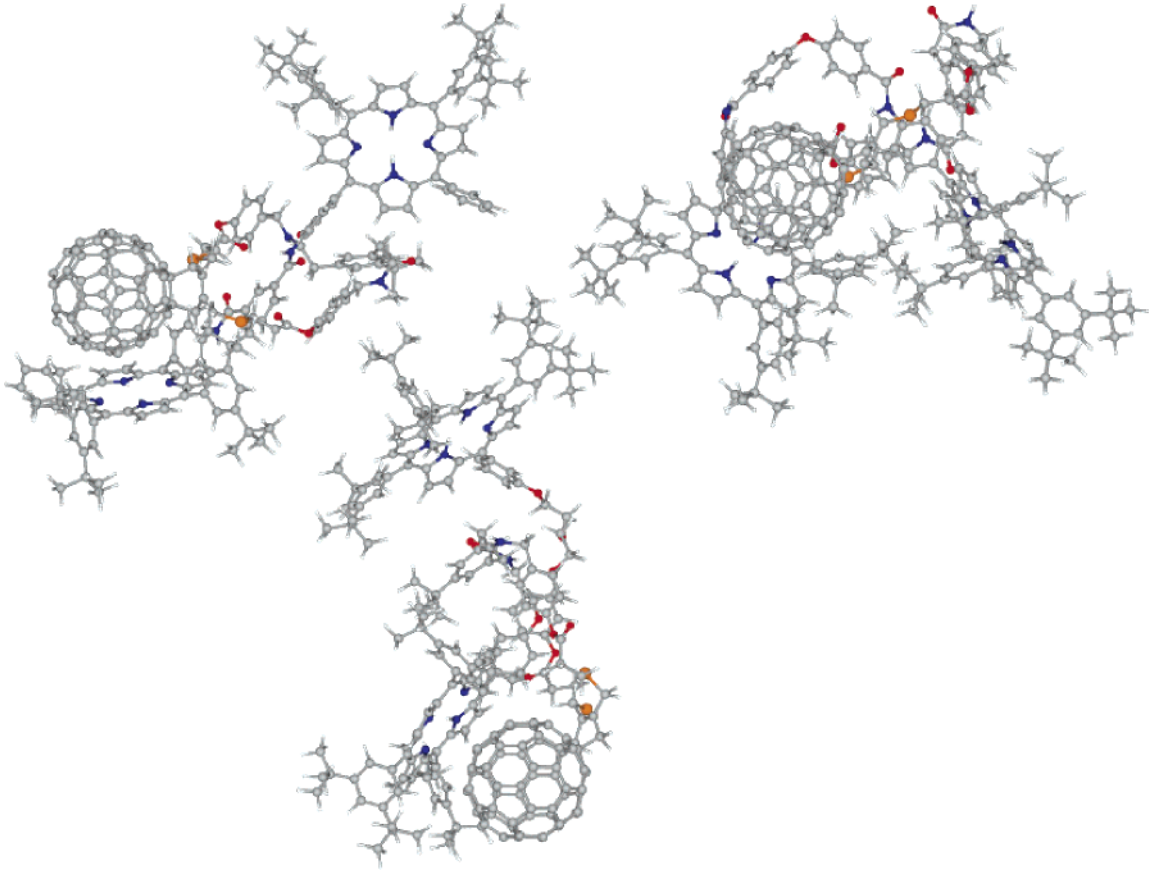

Figure 5. Optimized structures of rotaxanes **1a**−**c** calculated with probable R_{CC} values.

TABLE 1: Free-Energy Changes of Charge Separation (ΔG^{S}_{CS}) via ^{1}ZnP* and (ΔG^{T}_{CS}) via ^{3}ZnP* and Charge Recombination (ΔG_{CR}) of 1a, 1b, and 1c in PhCN, THF, and Toluene TN

sample	solvent	$-\Delta G^{S}_{CS}$/eV	$-\Delta G^{T}_{CS}$/eV	$-\Delta G_{CR}$[a]
1a	PhCN	0.85	0.25	1.25
1a	THF	0.79	0.19	1.31
1a	TN	0.58	−0.02	1.52
1b	PhCN	0.84	0.24	1.26
1b	THF	0.77	0.17	1.33
1b	TN	0.52	−0.08	1.58
1c	PhCN	0.82	0.22	1.28
1c	THF	0.73	0.13	1.37
1c	TN	0.45	−0.15	1.65

[a] $-\Delta G_{CR} = -E_{ox} + E_{red} - \Delta G_S$; and $\Delta G^{S,T}_{CS} = E_{o,o}$ (^{1}ZnP*, ^{3}ZnP*) $-\Delta G_{CR}$; for **1a**, $E_{ox} = 0.29$ V and $E_{red} = -1.10$ V, for **1b**, $E_{ox} = 0.26$ V and $E_{red} = -1.08$ V, and for **1c**, $E_{ox} = 0.28$ V and $E_{red} = -1.08$ V vs Fc/Fc$^+$ in PhCN. $E_{o,o}(^1\text{ZnP*}) = 2.10$ V and $E_{o,o}(^3\text{ZnP*}) = 1.50$ V, $\Delta G_S = e^2/(4\pi\epsilon_0))[(1/(2R_+) + 1/(2R_-) - 1/R_{CC})/\epsilon_S - (1/(2R_+) + 1/(2R_-))/\epsilon_R]$, where R_+, R_-, and R_{CC} are radii of cation (4.7 Å), anion (5.6 Å), and center-to-center distance between donor and acceptor (R_{CC} = 7.0, 7.5, and 8.1 Å for for **1a**, **1b**, and **1c**), respectively. The ϵ_S and ϵ_R are dielectric constants of solvents used for photophysical studies and for measuring the redox potentials, respectively.[34]

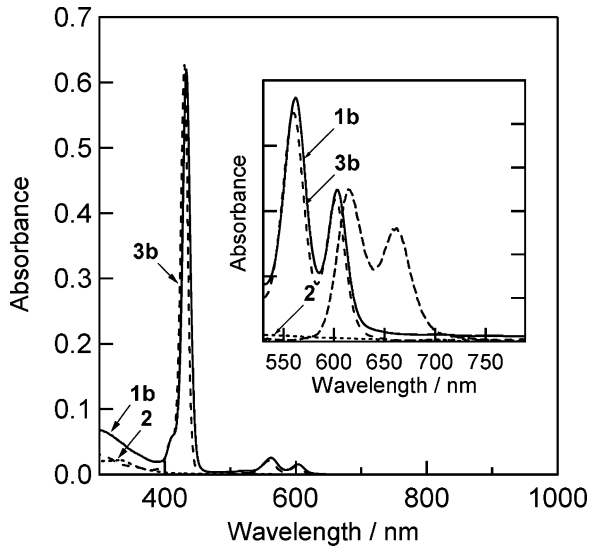

Figure 6. Steady-state absorption spectra of **1b**, **3b**, and **2** (0.001 mM) in PhCN. Inset: Steady-state absorption spectra of **1b**, **3b,** and **2** and fluorescence spectrum (dashed line) of **1b** (0.01 mM).

C_{60} ($C_{60}^{\bullet-}$) moiety;[41] the absorption bands at 700 and 880 nm were attributed to the triplet states of the C_{60} and ZnP moieties, with which the cation radical of the ZnP moieties (ZnP$^{\bullet+}$) in the 640−680 nm may overlap.[42] Similar results were also observed in THF and toluene. The inset time profile in Figure 8 shows the rapid rise and slow decay of the $C_{60}^{\bullet-}$ at 1000 nm. The absorption of the $C_{60}^{\bullet-}$ moiety at 1000 nm seems to rise immediately after laser light excitation at room temperature. This indicates that the CS process takes place via the ^{1}ZnP* moiety. In THF and toluene, similar transient spectra and time profiles were observed. Very similar observations were made for **1a**.[5a]

Figure 9 shows the nanosecond transient absorption spectra of **1c** in PhCN. The transient absorption band of the $C_{60}^{\bullet-}$ moiety appeared at 1000 nm,[41] while in the case of $^3C_{60}$* and ^{3}ZnP* moieties transient absorption bands were observed at 700 and 880 nm. In the absorption spectrum at 1.0 μs, the peak observed at 640−680 nm can be attributed to ZnP$^{\bullet+}$.[42] Similar results were observed in THF and toluene. The inset time profile at 1000 nm in Figure 9 shows the slow rise and decay of the $C_{60}^{\bullet-}$

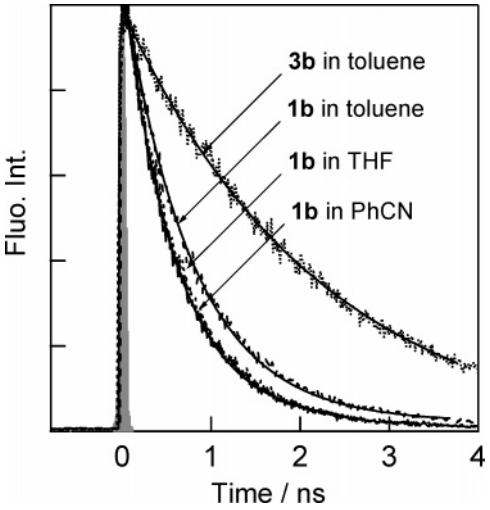

Figure 7. Time profiles of the fluorescence at 625 nm of rotaxane **1b** in PhCN, THF, and toluene (TN) and reference **3b** in toluene. Excitation wavelength was 410 nm at room temperature

TABLE 2: Fluorescence Lifetimes (τ_f), Rate Constants (k^S_{CS}), and Quantum Yields (Φ^S_{CS}) for Charge Separation via ^{1}ZnP* of Rotaxanes 1a, 1b, and 1c in PhCN, THF, and TN at Room Temperature

sample	solvent	τ_f/ps	$k^S_{CS}{}^a$/s^{-1}	$\Phi^S_{CS}{}^a$
1a	PhCN	90	1.1×10^{10}	0.95
1a	THF	120(40%)	7.3×10^9	0.93
		1800(60%)	$(3.1 \times 10^9)^b$	$(0.37)^b$
1a	TN	100(73%)	9.4×10^9	0.94
		1800(27%)	$(6.9 \times 10^9)^b$	$(0.67)^b$
1b	PhCN	680	9.0×10^8	0.61
1b	THF	680	9.0×10^8	0.61
1b	TN	860	5.9×10^8	0.51
1c	BN	1010	4.2×10^8	0.42
1c	THF	1040	4.3×10^8	0.46
1c	TN	1330	3.0×10^8	0.38

[a] Lifetimes (τ_{f0}) of reference were evaluated to be 1800 ps for **3a**, 1740 ps for **3b**, and 1740 ps for **3c** in PhCN, THF, and toluene. [b] Averaged values calculated from the fast and slow components.

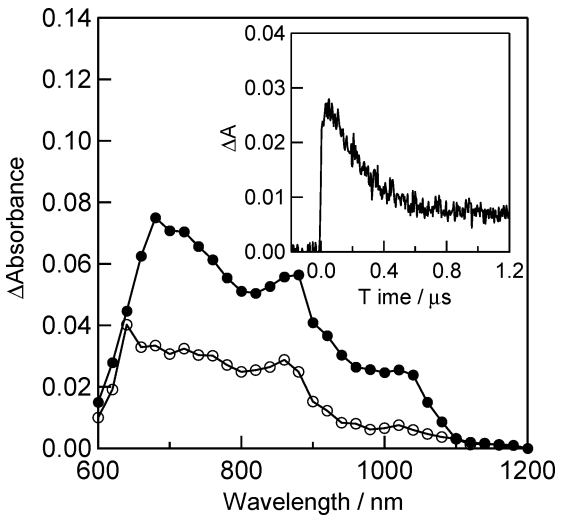

Figure 8. Nanosecond transient absorption spectra of **1b** (0.1 mM) observed by 532 nm laser irradiation in BN after 100 ns (●) and 1.0 μs (○). Inset: Trace of the C_{60} radical anion at 1000 nm at room temperature.

moiety. The absorption of the $C_{60}^{\bullet-}$ moiety at 1000 nm seems to rise slowly reaching maximum at 200−250 ns after laser light excitation at room temperature. This observation indicates that

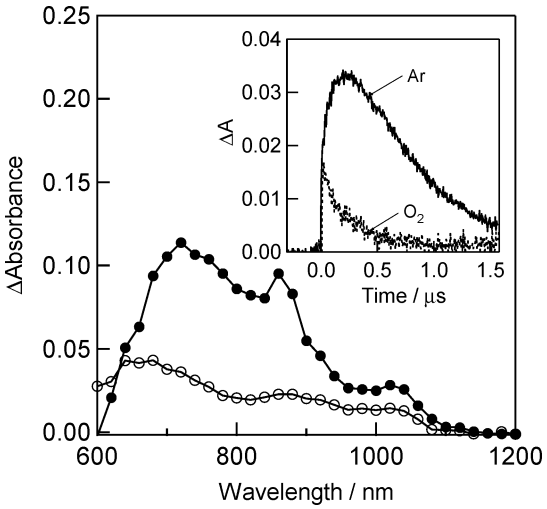

Figure 9. Nanosecond transient absorption spectra of **1c** (0.1 mM) observed by 532 nm laser irradiation in BN after 100 ns (●) and 1.0 μs (○). Inset: Time profiles of C_{60} radical anion at 1000 nm in Ar- and O_2-saturated PhCN at room temperature.

TABLE 3: Rate Constants (k^T_{CS}) and Quantum Yields (Φ^T_{CS}) at Room Temperature for Charge Separation via ^{3}ZnP* Rotaxanes 1a, 1b, and 1c in PhCN, THF, and TN

sample	solvent	$k^T_{CS}{}^a$/s^{-1}	$\Phi^T_{CS}{}^b$
1b	PhCN	2.3×10^8	0.48
1b	THF	2.1×10^8	0.46
1b	TN	$(3.4 \times 10^7)^c$	$(<0.2)^c$
1c	BN	5.0×10^7	0.32
1c	THF	2.5×10^7	0.42
1c	TN	$(1.2 \times 10^7)^c$	$(<0.2)^c$

[a] Calculated by following by the curve fitting of the rise at 1000 nm (Figure 9). [b] From $[C_{60}^{\bullet-}]/[^3\text{ZnP*}]$. $\epsilon_{880\ nm}(^3\text{ZnP*}) = 8500\ M^{-1}\ cm^{-1}$ and $\epsilon_{1000\ nm}(C_{60}^{\bullet-}) = 8400\ M^{-1}\ cm^{-1}$. [c] Mix with decay of ^{3}ZnP*.

the CS process takes place via the ^{3}ZnP* moiety. On addition of O_2, rapid decay of the $C_{60}^{\bullet-}$ moiety was observed, while pristine $C_{60}^{\bullet-}$ was not quenched by O_2. In THF and toluene, the transient spectra with a weak 1000 nm band may overlap with the absorption bands of $C_{60}^{\bullet-}$ via ^{3}ZnP* and via $^3C_{60}$*.

From the rise of the $C_{60}^{\bullet-}$ moiety, the rate constant (k^T_{CS}) for the CS process via ^{3}ZnP* was evaluated, as listed in Table 3 for **1b** and **1c**. From the ratio of $[C_{60}^{\bullet-}]/[^3\text{ZnP*}]$ in the observed transient absorption spectra, the quantum yield (Φ^T_{CS}) of the CS process via ^{3}ZnP* was also evaluated using the reported molar extinction coefficients (Table 3). Thus, the quantum yield vs the absorbed light can be evaluated from Φ^T_{CS} $(1 - \Phi^S_{CS})$. For example, the quantum yield vs the absorbed light for **1c** is 0.31 from Tables 2 and 3.

In Figures 8 and 9, the decays of the $C_{60}^{\bullet-}$ moiety at 1000 nm, which obeyed first-order kinetics with rate constants of $(1.0-3.8) \times 10^6\ s^{-1}$ in polar solvents, correspond to the CR rate constants (k_{CR}) as listed in Table 4. In Figure 8, the slow decay part in the 600−1000 ns may be attributed to the tail of the absorption of ^{3}ZnP* moiety. The k_{CR} values evaluated for **1b** and **1c** in toluene may be unreliable, because of overlapping with the slow decay of the triplet states. These k_{CR} values in PhCN and THF correspond to the lifetimes (τ_{RIP}) $(ZnP^{\bullet+},C_{60}^{\bullet+})_{rotaxane}$, which were evaluated in the 180−650 ns region, depending on interlocking structure and axle length; the τ_{RIP} values for **1c** with a long axle are comparable to the reported value for covalently connected C_{60}−ZnP (770 ns in PhCN at room temperature).[19] The solvent polarity effect on the τ_{RIP} values was not appreciable, as shown in Table 4. This is quite

TABLE 4: Rate Constants (k_{CR}) and Free Energies ($-\Delta G_{CS}$) of Charge Recombination and Lifetimes (τ_{RIP}) at Room Temperature of Radical Ion Pairs of 1a, 1b, and 1c in BN, THF, and TN

sample	solvent	k_{CR}/s^{-1}	τ_{RIP}/ns
1a	PhCN	5.5×10^6	180
1a	THF	4.4×10^6	230
1a	TN	3.8×10^6	260
1b	PhCN	4.3×10^6	230
1b	THF	3.9×10^6	250
1b	TN	$(1.4 \times 10^6)^a$	$(710)^a$
1c	PhCN	1.6×10^6	625
1c	THF	1.5×10^6	645
1c	TN	$(0.74 \times 10^6)^a$	$(1350)^a$

[a] Mix with decay of ^{3}ZnP*.

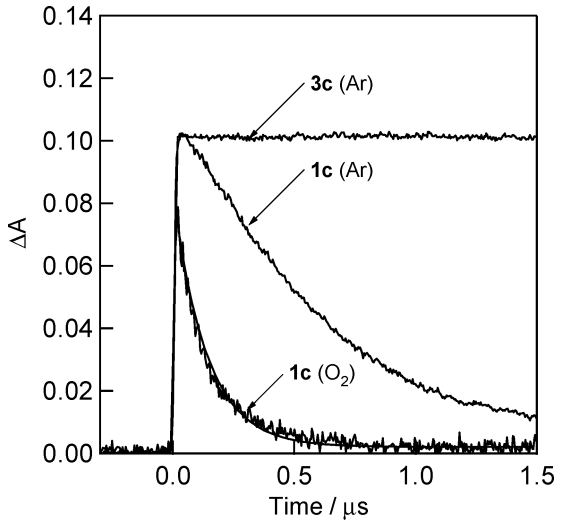

Figure 10. Absorption time profiles of the triplet state of ZnP of **1c** and reference compound **3c** (0.1 mM) at 880 nm in Ar- and O_2-saturated PhCN at room temperature.

different from the solvent polarity effect on the τ_{RIP} values for covalently connected dyads. For **1a**, the following tendency was observed: τ_{RIP} in PhCN < τ_{RIP} in THF < τ_{RIP} in toluene. For **1b** and **1c**, τ_{RIP} in PhCN is almost the same as τ_{RIP} in THF. In toluene, the τ_{RIP} values for **1b** and **1c** seem to be longer than those in polar solvent; however, this may be attributed to the overlapping of the absorption decay of the $C_{60}^{\bullet-}$ moiety with that of the ^{3}ZnP* moiety in toluene.

Figure 10 shows the observed time profile at 880 nm of the ^{3}ZnP* moiety of **1c** in PhCN, which decays faster compared with the lifetime of pristine ^{3}ZnP* (40−50 μs). The time profile at 880 nm due to the ^{3}ZnP* moiety of **1c** in PhCN is fairly similar to the decay of the $C_{60}^{\bullet-}$ moiety in **1c** at 1000 nm. This suggests that the ^{3}ZnP* moiety of **1c** is in equilibrium with $(ZnP^{\bullet+},C_{60}^{\bullet-})_{rotaxane}$. On addition of O_2, the ^{3}ZnP* moiety of **1c** in PhCN was quenched similarly to the $C_{60}^{\bullet-}$ moiety in **1c**.

Temperature Effect. With decreasing temperature, the rise of the $(ZnP^{\bullet+},C_{60}^{\bullet-})_{rotaxane}$ becomes slow as shown for **1b** in PhCN (Figure 11), indicating that the switching of the CS process takes place from the CS process via ^{1}ZnP* to the CS process via ^{3}ZnP* at low temperatures. From the rise, the k^T_{CS} value was evaluated to be 10^7 s^{-1} at 203 K. The decay of $(ZnP^{\bullet+},C_{60}^{\bullet-})_{rotaxane}$ slowed, indicating temperature dependence on the k_{CS} and k_{CR} values.

Figure 12 shows the temperature dependence of the k_{CR} values for **1b** in PhCN and THF; slight dependences were observed for all rotaxanes.[43] The Gibbs activation energies for the CR process ($\Delta G^{\ddagger}_{CR}$) in **1a**−**c** were evaluated in the 0.06−0.08 eV

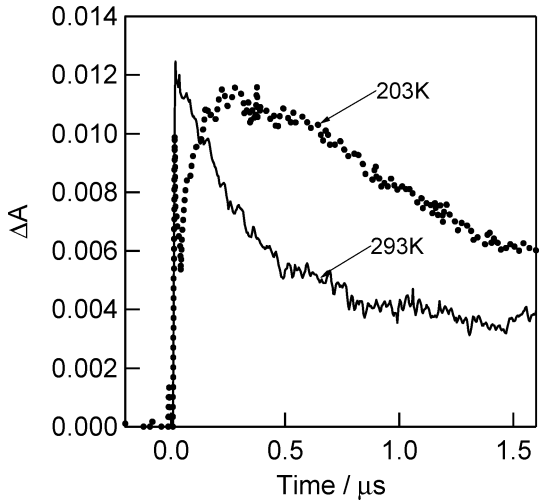

Figure 11. Time profiles of the C_{60} radical anion at 1000 nm in **1b** at room temperature and low temperature in THF.

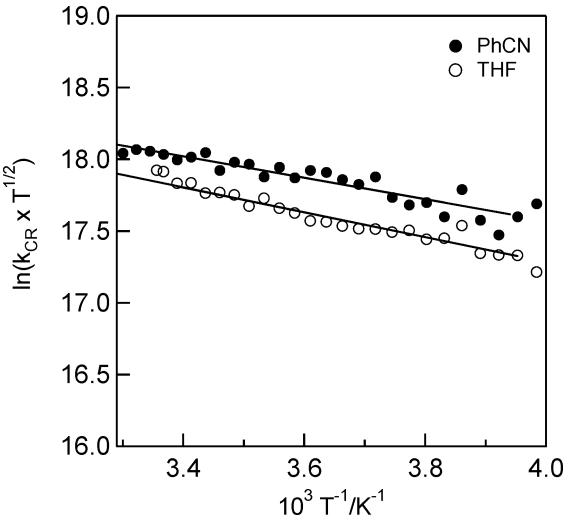

Figure 12. Modified Arrhenius plots of the temperature-dependent k_{CR} for rotaxane **1b** in PhCN (●) and THF (○).

region, which are quite smaller than the $\Delta G^{\ddagger}_{CR}$ values of covalently connected dyad systems such as the retinyl−C_{60} (0.16 eV)[14c,44] and diphenylamine-substituted fluorene−C_{60} dyad (0.11 eV).[23] In general, the $\Delta G^{\ddagger}_{CR}$ values for through-space electron transfer are expected to be almost zero, while considerably higher $\Delta G^{\ddagger}_{CR}$ values are anticipated for through-bond electron transfer. Thus, the small $\Delta G^{\ddagger}_{CR}$ values observed for rotaxane **1a**, **1b**, and **1c** support the assumption that the CR process takes place via through-space electron transfer.

From similar plots for the k^T_{CS} values (Supporting Information, Figure S2), the Gibbs activation energy for the CS process via ^{3}ZnP* ($\Delta G^{\ddagger T}_{CS}$) was evaluated to be less than 0.07 eV, showing resemblance with the CR process. Nonzero values of $\Delta G^{\ddagger}_{ET}$ of **1a**, **1b**, and **1c** can be attributed to the flexibility of the relative configuration of the ZnP and C_{60} moieties. Such molecular mobility of the rotaxanes **1a**−**c** were estimated from the molecular dynamics, as shown in Figure 4.

Energy Diagrams. The energy diagram for the charge separation and recombination processes after the photoexcitation of the ZnP moiety is shown in Figure 13. The energies of the radical ion pair states for rotaxanes **1a**, **1b**, and **1c** are shown in Table 1. The shortening of fluorescence lifetimes indicates that charge separation takes place mainly from the ^{1}ZnP* moiety producing $(ZnP^{\bullet+},C_{60}^{\bullet-})_{rotaxane}$ in polar and nonpolar solvents;

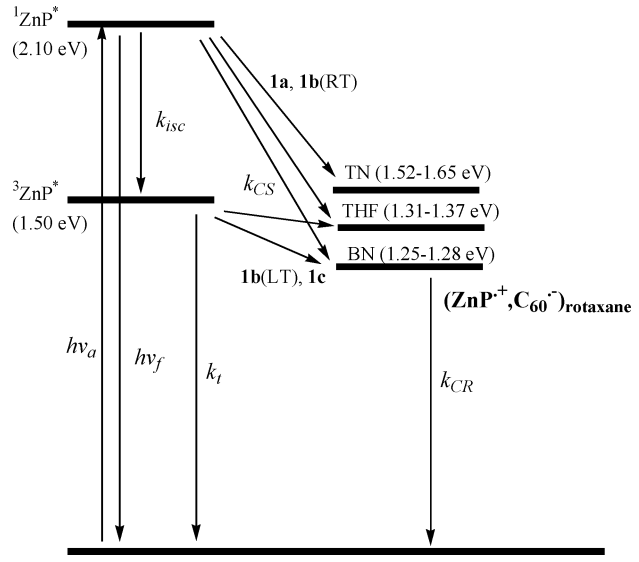

Figure 13. Energy levels and electron-transfer paths via ^{1}ZnP* of **1a**, **1b**, and **1c** in PhCN, THF, and TN (toluene): RT, room temperature; LT, low temperature.

however, the rate and efficiency of the charge-separation process depend on the axle length (or more exactly R_{CC}). In polar solvents, the CS process via the ^{3}ZnP* moiety producing $(ZnP^{\bullet+},C_{60}^{\bullet-})_{rotaxane}$ is possible, while in nonpolar solvent this process was not clearly confirmed due to the overlap of the absorption of the $C_{60}^{\bullet-}$ with that of the ^{3}ZnP* moiety; indeed, the ΔG^T_{CS} values are slightly positive in toluene. The slow recombination rates suggest that the free energies of the CR process lie in an inverted region far more negative than the λ_{CR} values.

Conclusions

Three new C_{60}-containing rotaxanes carrying porphyrin moieties at the axle termini with different axle lengths were synthesized via preorganization using hydrogen bonding between the amide groups of the wheel and the axle. The introduction of the C_{60} moiety into the rotaxanes was performed via the Diels−Alder reaction between the sulfolene-functionalized wheel and C_{60} in ca. 70% yield. Switching of the CS process takes place from the excited singlet route to the excited triplet route depending on axle length. Similar switching of the CS process takes place with the lowering of temperature. This interchange may also be affected by the mobility of the donor and acceptor moieties spatially positioned in the rotaxanes. Low activation energies for the CS process via ^{3}ZnP* and the CR process were evaluated. All of these phenomena are characteristic of through-space electron transfer in rotaxanes.

Experimental Section

Molecular Dynamics Calculations. All of the calculations were performed by the MM3 force field as modified in the MacroModel package.[38]

Electrochemical Measurements. The cyclic voltammetry measurements were performed on a BAS CV-50 W electrochemical analyzer in deaerated PhCN solution (sample concentration = ca. 5.0×10^{-4} M) containing 0.10 M tetra-*n*-butylammonium perchlorate as a supporting electrolyte at 298 K (100 mV s^{-1}). The glassy carbon was used as a working electrode, and the counter electrode was a platinum wire. The measured potentials were recorded with respect to an Ag/AgCl reference electrode (saturated KCl) and calculated with Fc/Fc^+ as an internal standard.

Spectral Measurements. Time-resolved fluorescence spectra were measured by a single-photon-counting method using a second harmonic generation (SHG, 410 nm) of a Ti:sapphire laser (Spectra-Physics, Tsunami 3950-L2S, 1.5 ps full width at half-maximum (fwhm)) and a streak scope (Hamamatsu Photonics, C4334-01) equipped with a polychromator (Action Reasearch, SpectraPro 150) as an excitation source and a detector, respectively.

Nanosecond transient absorption measurements were carried out using a SHG (532 nm) of a Nd:YAG laser (Spectra-Physics, Quanta-Ray GCR-130, fwhm 6 ns) as an excitation source. For transient absorption spectra in the near-IR region (600−1600 nm), monitoring light from a pulsed Xe lamp was detected with a Ge-avalanche photodiode (Hamamatsu Photonics, B2834). Photoinduced events in micro- and millisecond time regions were estimated by using a continuous Xe lamp (150 W) and an InGaAs-PIN photodiode (Hamamatsu Photonics, G5125-10) as a probe light and a detector, respectively. Details of the transient absorption measurements were described elsewhere.[45,46] All of the samples in a quartz cell (1×1 cm) were deaerated by bubbling argon through the solution for 15 min.

Synthesis of Rotaxanes. *General Information.* Melting points were measured on a Yanaco micro melting-point apparatus and were uncorrected. IR spectra were recorded on a Jasco FT-IR model 230 spectrometer. ^{1}H NMR (400 MHz) and ^{13}C NMR (100 MHz) measurements were performed on a JEOL JMN-LA-400 spectrometer, where the chemical shifts were represented as δ values relative to an internal standard TMS or solvent peak. Preparative SEC was carried out on a JAI LC-918 system using a JAIGEL-1 column eluted by chloroform. FAB-MS was measured by a Finigan TSQ-70 instrument. All commercially available reagents and solvents were used without further purification unless noted. For the preparation of rotaxane, amylene-stabilized $CHCl_3$ was used.

*Rotaxane **7a.*** To a solution of 4,10,15-tris(3,5-di-*tert*-butylphenyl)-20-(4-aminophenyl)-porphyrin (**6**)[33] (390 mg, 0.40 mmol) and triethylamine (40 mg, 0.4 mmol) in $CHCl_3$ (20 mL) was added a solution of macrocycle **4**[31] (72 mg, 0.10 mmol) and **5a** (20 mg, 0.10 mmol) in $CHCl_3$ (20 mL) over a period of 1 h at 0 °C. An additional $CHCl_3$ solution (10 mL) of **5a** (20 mg, 0.10 mmol) was then added over a period of 1 h at 0 °C. The mixture was stirred at room temperature for 5 h and evaporated to dryness. The residue was purified by silica gel chromatography (eluent, $CHCl_3$), then preparative HPLC to afford **7a** (46 mg, 17% yield based on the macrocycle **4**) as a black-purple solid. Mp: >300 °C. IR (KBr): 3317, 2962, 1652, 1592, 1520, 1247, 802 cm^{-1}. ^{1}H NMR (400 MHz, $CDCl_3$): δ 9.12 (s, 1H), 8.89 (d, J = 4.9 Hz, 4H), 8.93 (s, 8H), 8.90 (d, J = 4.9 Hz, 4H), 8.81 (s, 1H), 8.40 (s, 2H), 8.24 (d, J = 8.3 Hz, 4H), 8.11 (s, 8H), 8.09 (s, 4H), 8.00 (br s, 2H), 7.96 (d, J = 8.1 Hz, 4H), 7.81 (m, 6H), 7.62 (t, J = 8.2 Hz, 1H), 7.11 (d, J = 8.3 Hz, 4H), 6.73 (d, J = 8.3 Hz, 4H), 4.61 (s, 4H), 4.08 (s, 4H), 4.02 (s, 4H), 3.37 (s, 4H), 1.54 (s, 108H), 1.30 (s, 9H), −2.66 (br s, 4H) ppm. FAB-MS (matrix, *m*NBA): *m*/*z* 2784 $[(M + H)^+]$.

*Rotaxane **3a.*** To a solution of **7a** (10 mg, 3.6 μmol) in $CHCl_3$ (50 mL) was added a saturated methanol solution (2 mL) of zinc acetate, and the mixture was refluxed for 30 min. After being cooled, the reaction mixture was washed by water, dried over anhydrous Na_2SO_4, and evaporated. The residue was purified by chromatography over silica gel (eluent, $CHCl_3$) and further purified by preparative HPLC to afford **3a** (9 mg, 86%)

as a black-purple solid. Mp: >300 °C. IR (KBr): 3348, 2962, 1652, 1592, 1520, 1248, 797 cm^{-1}. ^1H NMR (400 MHz, $CDCl_3$): δ 9.11 (s, 1H), 9.08 (d, $J = 4.5$ Hz, 4H), 9.02 (s, 8H), 8.99 (d, $J = 4.5$ Hz, 4H), 8.75 (s, 2H), 8.40 (s, 1H), 8.37 (s, 2H), 8.23 (d, $J = 8.4$ Hz, 4H), 8.13−8.09 (m, 14H), 7.99 (t, $J = 5.0$ Hz, 2H), 7.94 (d, $J = 8.4$ Hz, 4H), 7.80 (s, 6H), 7.65 (t, $J = 7.6$ Hz, 1H), 7.12 (d, $J = 8.8$ Hz, 4H), 6.74 (d, $J = 8.8$ Hz, 4H), 4.59 (s, 4H), 4.07 (s, 4H), 4.00 (s, 4H), 3.37 (s, 4H), 1.53 (s, 108H), 1.29 (s, 9H) ppm. FAB-MS (matrix, *m*NBA): *m*/*z* 2844 [$(M - SO_2 + H)^+$]. Anal. Calcd for $C_{180}H_{194}N_{12}O_{10}S_3Zn_2 \cdot H_2O \cdot 3CHCl_3$: C, 70.45; H, 6.57; N, 5.45. Found: C, 70.59; H, 6.48; N, 5.60.

Rotaxane ***8a.*** A mixture of C_{60} (47 mg, 65 μmol), **7a** (35 mg, 13 μmol), and hydroquinone (0.5 mg) in 1,2-dichlorobenzene (15 mL) was refluxed for 1.5 h. After being cooled, the reaction mixture was evaporated to dryness. The residue was passed over silica gel using $CHCl_3$ as an eluent, and the product was purified by preparative HPLC to afford **8a** (30 mg, 69%) as a black-purple solid. Mp: >300 °C (decomposition). IR (KBr): 3373, 2962, 1650, 1519, 1505, 1247 cm^{-1}. ^1H NMR (400 MHz, $CDCl_3$, 328 K): δ 9.21 (s, 1H), 8.99 (s, 2H), 8.88−8.79 (m, 17H), 8.54 (s, 1H), 8.42 (s, 2H), 8.11−7.72 (m, 30H), 7.08 (d, $J = 8.3$ Hz, 4H), 6.79 (d, $J = 8.3$ Hz, 4H), 4.57 (br, 4H), 4.14 (br, 4H), 3.63 (br, 4H), 3.49 (s, 4H), 1.53 (s, 36H), 1.48 (s, 72H), 1.37 (s, 9H), −2.79 (br, 4H) ppm. FAB-MS (matrix, *m*NBA): *m*/*z* 3441 [$(M + H)^+$].

Rotaxane ***1a.*** The compound was synthesized from **8a** by the same manner as mentioned for the synthesis of **3a**. **1a** was obtained (82%) as a black-purple solid. Mp: >300 °C. IR (KBr) 3350, 2961, 1652, 1538, 1520, 1505 cm^{-1}. ^1H NMR (400 MHz, $CDCl_3$, 328 K): δ 9.18 (s, 1H), 8.97−8.89 (m, 20H), 8.54 (s, 1H), 8.38 (s, 2H), 8.10−7,99 (m, 22H), 7.78 (t, $J = 1.7$ Hz, 2H), 7.76 (t, $J = 1.7$ Hz, 4H), 7.72 (t, $J = 7.8$ Hz, 1H), 7.07 (d, $J = 8.5$ Hz, 4H), 6.69 (d, $J = 8.5$ Hz, 4H), 4.54 (br, 4H), 4.15 (br, 4H), 3.63 (br, 4H), 3.49 (s, 4H), 1.53 (s, 36H), 1.49 (s, 72H), 1.35 (s, 9H) ppm. FAB-MS (matrix, *m*NBA): *m*/*z* 3564 [$(M + H)^+$]. Anal. Calcd for $C_{240}H_{194}N_{12}O_8S_2Zn_2 \cdot 6H_2O$: C, 78.39; H, 5.65; N, 4.57. Found: C, 78.45; H, 5.64; N, 4.61

Acknowledgment. This present work was supported by a Grant-in-Aid for Scientific Research in Priority Areas (417) from the Ministry of Education, Culture, Sports, Science and Technology of Japan (12875163 and 14050014).

Supporting Information Available: Experimental procedures and characterization data for rotaxanes **1b**, **1c**, **3b**, **3c**, **7b**, **7c**, **8b**, and **8c**, cyclic voltamographs, and temperature dependence of the k^T_{CS} values. This material is available free of charge via the Internet at http://pubs.acs.org.

References and Notes

(1) *Molecular Catenanes, Rotaxanes and Knots*; Sauvage, J.-P., Dietrich-Buchecker, C., Eds.; Wiley-VCH: Weinheim, Germany 1999.

(2) (a) Amabilino, D. B.; Stoddart, J. F. *Chem. Rev.* **1995**, *95*, 2725. (b) Chambron, J.-C.; Sauvage, J.-P. *Chem.—Eur. J.* **1998**, *4*, 1362. (c) Nepogodiev, S. A.; Stoddart, J. F. *Chem. Rev.* **1998**, *98*, 1959. (d) Balzani, V.; Credi, A.; Raymo, F. M.; Stoddart, J. F. *Angew. Chem., Int. Ed.* **2000**, *39*, 3349. (e) Hubin, T. J.; Busch, D. H. *Coord. Chem. Rev.* **2000**, *200*, 5, 1172.

(3) (a) Kawasaki, H.; Kihara, N.; Takata, T. *Chem. Lett.* **1999**, 1015. (b) Furusho, Y.; Oku, T.; Hasegawa, T.; Tsuboi, A.; Kihara, N.; Takata, T. *Chem.—Eur. J.* **2003**, *9*, 2895.

(4) Tachibana, Y.; Kihara, N.; Takata, T. *J. Am. Chem. Soc.* **2004**, *126*, 3438.

(5) (a) Watanabe, N.; Kihara, N.; Furusho, Y.; Takata, T.; Araki, Y.; Ito, O. *Angew. Chem., Int. Ed.* **2003**, *42*, 681. (b) Sandanayaka, A. S. D.; Sasabe, H.; Araki, Y.; Furusho, Y.; Ito, O.; Takata, T. *J. Phys. Chem. A* **2004**, *108*, 5145.

(6) (a) Wang, Y. *Nature* **1992**, *356*, 585. (b) Wang, Y.; West, R.; Yuan, C.-H. *J. Am. Chem. Soc.* **1993**, *115*, 3844.

(7) (a) Hawng, K. C.; Mauzerall, D. *J. Am. Chem. Soc.* **1992**, *114*, 9705. (b) Hwang, K. C.; Mauzerall, D. *Nature* **1993**, *361*, 138.

(8) (a) Yoshino, K.; Xiao, H.; Nuro, K.; Kiyomatsu, S.; Morita, S.; Zakihdov, A. A.; Noguchi, T.; Ohnishi, T. *Jpn. J. Appl. Phys.* **1993**, *32*, L357. (b) Kepler, R. G.; Gahill, P. A. *Appl. Phys. Lett.* **1993**, *63*, 1552. (c) Kraabel, B. D.; McBranch, D.; Saricifici N. S.; Moses, D.; Heeger, A. J. *Phys. Rev. B* **1994**, *50*, 18543. (d) Chen, W. X.; Xu, Z. D.; Li, W. Z. *J. Photochem. Photobiol., A* **1995**, *68*, 179. (e) Murata, K.; Ito, S.; Takahashi, K.; Hoffman, B. *Appl. Phys. Lett.* **1996**, *68*, 427. (f) Yonehara, H.; Pac, C. *Thin Solid Films* **1966**, *276*, 108. (g) Schlebusch, C.; Kessler, B.; Cramm, S.; Eberhart, W. *Synth. Met.* **1966**, *77*, 151. (h) Milanesio, M. E.; Gervaldo, M.; Otero, L. A.; Sereno, L.; Silber, J. J.; Durantin, E. N. *J. Phys. Org. Chem.* **2002**, *15*, 44.

(9) (a) Nojiri, T.; Alam, M. M.; Konami, H.; Watanabe, A.; Ito, O. *J. Phys. Chem. A* **1997**, *101*, 7943. (b) Nojiri, T.; Watanabe, A.; Ito, O. *J. Phys. Chem. A* **1998**, *102*, 5215. (c) El-Khouly, M. E.; Fujitsuka, M.; Ito, O. *J. Porphyrins Phthalocyanines* **2000**, *4*, 591. (d) El-Khouly, M. E.; Islam, S. D-M.; Fujitsuka, M.; Ito, O. *J. Porphyrins Phthalocyanines* **2000**, *4*, 713. (e) El-Khouly, M. E.; Araki, Y.; Fujitsuka, M.; Ito, O. *Photochem. Photobiol.* **2001**, *74*, 22. (f) El-Khouly, M. E.; Fujitsuka, M.; Ito, O. *Phys. Chem. Chem. Phys.* **2002**, *4*, 3322.

(10) (a) Guldi, D. M.; Neta, P.; Asmus, K.-D. *J. Phys. Chem.* **1994**, *98*, 4617. (b) Martino, D. M.; van Willigen, H. *J. Phys. Chem. A* **2000**, *104*, 10701.

(11) (a) Fujisawa, Y.; Yasunori, O.; Yamauchi, S. *Chem. Phys. Lett.* **1998**, *282*, 181. (b) Fujisawa, Y.; Yasunori, O.; Yamauchi, S. *Chem. Phys. Lett.* **1998**, *294*, 248.

(12) (a) Sension, R. J.; Szarka, A. Z.; Smith, A. B., III; Hochstrasser, R. M. *Chem. Phys. Lett.* **1991**, *185*, 179. (b) Palit, D. K.; Ghosh, H. N.; Pal, H.; Sapre, A. V.; Mittal, J. P.; Seshadri, R.; Rao, C. N. R. *Chem. Phys. Lett.* **1992**, *198*, 113. (c) Park, J.; Kim, D.; Suh, Y. D.; Kim, S. K. *J. Phys. Chem.* **1994**, *98*, 12715.

(13) (a) Imahori, H.; Sakata, Y. *Adv. Mater.* **1997**, *9*, 537. (b) Imahori, H.; Yamada, K.; Hasegawa, M.; Taniguchi, S.; Okada, T.; Sakata, Y. *Angew. Chem., Int. Ed. Engl.* **1997**, *36*, 2626. (c) Imahori, H.; Sakata, Y. *Eur. J. Org. Chem.* **1999**, 2445. (d) Luo, C.; Guldi, D. M.; Imahori, H.; Tamaki, K.; Sakata, Y. *J. Am. Chem. Soc.* **2000**, *122*, 6535. (e) Imahori, H.; Tamaki, K.; Guldi, D M.; Luo, C.; Fujitsuka, M.; Ito, O.; Sakata, Y.; Fukuzumi, S. *J. Am. Chem. Soc.* **2001**, *123*, 2607. (f) Imahori, H.; Guldi, D M.; Tamaki, K.; Yoshida, Y.; Luo, C.; Sakata, Y.; Fukuzumi, S. *J. Am. Chem. Soc.* **2001**, *123*, 6617. (g) Imahori, H.; Tamaki, K.; Guldi, D. M.; Luo, C.; Fujitsuka, M.; Ito, O.; Sakata, Y.; Fukuzumi, S. *J. Am. Chem. Soc.* **2001**, *123*, 2607. (h) Imahori, H.; Tamaki, K.; Araki, Y.; Sekiguchi, Y.; Ito, O.; Sakata, Y.; Fukuzumi, S. *J. Am. Chem. Soc.* **2002**, *124*, 5165. (i) Imahori, H.; Mori, Y.; Matano, J. *J. Photochem. Photobiol., C* **2003**, *4*, 51.

(14) (a) Guldi, D. M.; Prato, M. *Acc. Chem. Res.* **2000**, *33*, 695. (b) Guldi, D. M. *Chem. Soc. Rev.* **2002**, *31*, 22. (c) Guldi, D. M. *Chem. Commun.* **2000**, 321. (d) Guldi, D. M.; Hirsch, A.; Schloske, M.; Dietel, E.; Troisi, A.; Zerbetto, F.; Prato, M. *Chem.—Eur. J.* **2003**, *9*, 4968.

(15) (a) Tkachenko, N. V.; Rantala, L.; Tauber, A. Y.; Helaja, J.; Hynninen, P. H.; Lemmetyinen, H. *J. Am. Chem. Soc.* **1999**, *121*, 9378. (b) Tkachenko, N. V.; Tauber, A. Y.; Grandell, D.; Hynninen, P. H.; Lemmetyinen, H. *J. Phys. Chem. A* **1999**, *103*, 34646. (c) Vehmanen, V.; Tkachenko, N. V.; Imahori, H.; Fukuzumi, S.; Lemmetyinen, H. *Spectrochim. Acta, Part A* **2001**, *57*, 2229. (d) Kesti, T. J.; Tkachenko, N. V.; Vehmanen, V.; Yamada, H.; Imahori, H.; Fukuzumi, S.; Lemmetyinnen, H. *J. Am. Chem. Soc.* **2002**, *124*, 8067.

(16) Schuster, D. L.; Cheng, P.; Wilson, S. R.; Prokhorenko, V.; Katterle, M.; Holzwarth, A. R.; Braslavsky, S. E.; Klihm, G.; Williams, R. M.; Luo, C. *J. Am. Chem. Soc.* **1999**, *121*, 11599.

(17) (a) Linssen, T. G.; Durr, K.; Hannack, M.; Hirsh, A. *J. Chem. Soc., Chem. Commun.* **1995**, 103. (b) Durr, K.; Fiedler, S.; Linssen, T.; Hirshi, A.; Hanack, M. *Chem. Ber.* **1997**, *130*, 1375. (c) Saster, A.; Gouloumis, A.; Vazques, P.; Torres, T.; Doan, V.; Schwartz, B. J.; Wudl, F.; Echigoye, L.; Rivera, J. *Org. Lett.* **1999**, *1*, 1807. (d) Guldi, D. M.; Ramey, J.; Martinez-Diaz, M. V.; de la Escosura, A.; Torres, T.; Da Ros, T.; Prato, M. *Chem. Commun.* **2002**, 2774.

(18) Meijer, M. D.; van Klink, G. P. M.; van Koten, G. *Coord. Chem. Rev.* **2002**, *230*, 141.

(19) Imahori, H.; El-Khouly, M. E.; Fujitsuka, M.; Ito, O.; Sakata, Y.; Fukuzumi, S. *J. Phys. Chem. A* **2001**, *105*, 325.

(20) (a) Fujitsuka, M.; Ito, O.; Imahori, H.; Yamada, K.; Yamada, H.; Sakata, Y. *Chem. Lett.* **1999**, 721. (b) Imahori, H.; Tamaki, K.; Araki, Y.; Hasobe, T.; Ito, O.; Shimomura, A.; Kundu, S.; Okada, T.; Sakata, Y.; Fukuzumi, S. *J. Phys. Chem. A* **2002**, *106*, 1465. (c) Imahori, H.; Tamaki, K.; Araki, Y.; Sekuguchi, Y.; Ito, O.; Sakata, Y.; Fukuzumi, S. *J. Am. Chem. Soc.* **2002**, *124*, 5165.

(21) (a) Liddell, P. A.; Kuciauskas, D.; Sumida, J. P.; Nash, B.; Nguyen, D.; Moore, A. L.; Moore, T. A.; Gust, D. *J. Am. Chem. Soc.* **1997**, *119*, 1400. (b) Liddell, P. A.; Kodis, G.; Moore, A. L.; Moore, T. A.; Gust, D. *J. Am. Chem. Soc.* **2002**, *124*, 7668. (c) Smirnov, S. N.; Liddell, P. A.;

Vlassiouk, I. V.; Teslja, A.; Kuciauskas, D.; Braun, C. L.; Moore, A. L.; Moore, T. A.; Gust, D. *J. Phys. Chem. A* **2003**, *107*, 7567.

(22) Choi, M. S.; Aida, T.; Luo, H.; Araki, Y.; Ito, O. *Angew. Chem., Int. Ed.* **2003**, *42*, 4060.

(23) (a) Armaroli, N.; Diederich, F.; Echogeyen, L.; Habicher, T.; Flamigni, L.; Marconi, G.; Nierengarten, J.-F. *New J. Chem.* **1999**, *23*, 77. (b) Diederich, F.; Lopez, M. G. *Chem. Soc. Rev.* **1999**, *28*, 263. (c) Piotrowiak, P. *Chem. Soc. Rev.* **1999**, *28*, 143. (c) Armaroli, N.; Marconi, G.; Echogeyen, L.; Bourgleois, J.-P.; Diederich, F. *Chem.—Eur. J.* **2000**, *6*, 1629. (d) Guldi, D. M.; Luo, C.; Da Ros, T.; Prato, M.; Dietel, E.; Hirsch, A. *Chem. Commun.* **2000**, 375. (e) Da Ros, T.; Prato, M.; Guldi, D. M.; Ruzzi, M.; Pasimeni, L. *Chem.—Eur. J.* **2001**, *7*, 816. (f) Guldi, D. M.; Luo, C.; Swartz, A.; Scheloske, M.; Hirsch, A. *Chem. Commun.* **2001**, 1066. (g) Yin, G.; Xu, D.; Xu, Z. *Chem. Phys. Lett.* **2002**, *365*, 232. (h) Solladie, N.; Walther, M. E.; Cross, M.; Duartè, T. M. F.; Bougogne, C. T. M.; Nierengarten, J.-F. *Chem. Commun.* **2003**, 2412. (i) Weinkauf, J. R.; Cooper, S. W.; Schweiger, A.; Wamser, C. C. *J. Phys. Chem. A* **2003**, *107*, 3486. (j) Guldi, D. M.; Imahori, H.; Tamaki, K.; Kashiwagi, Y.; Yamada, H.; Sakata, Y.; Fukuzumi, S. *J. Phys. Chem. A* **2004**, *108*, 541.

(24) (a) D'Souza, F.; Deviprasad, G. R.; El-Khouly, M. E.; Fujitsuka, M.; Ito, O. *J. Am. Chem. Soc.* **2001**, *123*, 5277. (b) D'Souza, F.; Deviprasad, G. R.; Zandler, M. E.; Hoang, V. T.; Arkady, K.; Van Stipdonk, M.; Perera, A.; El-Khouly, M. E.; Fujitsuka, M.; Ito, O. *J. Phys. Chem. A* **2002**, *106*, 3243.

(25) D'Souza, F.; Deviprasad, G. R.; Zandler, M. E.; El-Khouly, M. E.; Fujitsuka, M.; Ito, O. *J. Phys. Chem. A* **2003**, *107*, 4801.

(26) (a) Li, K.; Schuster, D. I.; Guldi, D. M.; Herranz, M. A.; Echegoyen, L. *J. Am. Chem. Soc.* **2004**, *126*, 3388. (b) Schuster, D. I.; Li, K.; Guldi, D. M.; Raney, J. *Org. Lett.* **2004**, *6*, 1919. (c) Li, K.; Bracher, P. J.; Guldi, D. M.; Herranz, M. A.; Echegoyen, L.; Schuster, D. I. *J. Am. Chem. Soc.* **2004**, *126*, 9156.

(27) (a) Blanco, M. J.; Jimenez, M. C.; Chambron, J.-C.; Heitz, V.; Linke, M.; Sauvage, J.-P. *Chem. Soc. Rev.* **1999**, *28*, 293. (b) Andersson, M.; Linke, M.; Chanbron, J.-C.; Davidsson, J.; Heitz, V.; Sauage, J.-P.; Hammarstrom, L. *J. Am. Chem. Soc.* **2000**, *122*, 3526.

(28) Martinez-Diaz, M. V.; Fender, N. S.; Rodriguez-Morgade, M. S.; Gomes-Lopes, M.; Dietrich, F.; Echioyen, L.; Stoddart, J. F.; Torres, T. *J. Mater. Chem.* **2002**, *12*, 2095.

(29) (a) *The Photosynthetic Reaction Center*; Deisenhofer, J., Norris, J. R., Eds.; Academic Press: San Diego, 1993. (b) Deisenhofer, J.; Epp, O.; Miki, K.; Huber, R.; Michel, H. *J. Mol. Biol.* **1984**, *180*, 385. (c) Wasielewski, M. R.; Wiederrecht, G. P.; Svec, W. A.; Niemczyk, M. P. *Sol. Energy Mater. Sol. Cells* **1995**, *38*, 127.

(30) (a) Jäger, R.; Vögtle, F. *Angew. Chem., Int. Ed.* **1997**, *36*, 930. (b) Vögtle, F.; Dünnwald, T.; Schmidt, T. *Acc. Chem. Res.* **1996**, *29*, 451.

(31) Watanabe, N.; Kihara, H.; Takata, T. *Org. Lett.* **2001**, *3*, 3519.

(32) *Sulphones in Organic Synthesis*; Simpkins, N. S., Ed.; Pergamon: Oxford, 1993.

(33) Imahori, H.; Hagiwara, K.; Aoki, M.; Akiyama, T.; Taniguchi, S.; Okada, T.; Shirakawa, M.; Sakata, Y. *J. Am. Chem. Soc.* **1996**, *118*, 11771.

(34) The effects of the structures of diacid chlorides and diamines on the effectiveness in the rotaxane syntheses in the presence of macrolactam **3** will be reported elsewhere.

(35) (a) Furusho, Y.; Shoji, J.; Watanabe, N.; Kihara, N.; Adachi, T.; Takata, T. *Bull. Chem. Soc. Jpn.* **2001**, *74*, 139. (b) Watanabe, N.; Furusho, Y.; Kihara, N.; Takata, T.; Kinbara, K.; Saigo, K. *Bull. Chem. Soc. Jpn.* **2001**, *74*, 149.

(36) (a) An, Y.-Z.; Anderson, J. L.; Rubin, Y. *J. Org. Chem.* **1993**, *58*, 4799. (b) Ohno, M.; Kojima, S.; Shirakawa, Y.; Eguchi, S. *Tetrahedron Lett.* **1995**, *36*, 6899. (c) Torres-Garcia, G.; Luftmann, H.; Wolff, C.; Matty, J. *J. Org. Chem.* **1997**, *62*, 2752.

(37) We could not obtain high-quality ^{13}C NMR spectra of **1a** and **1b** because their conformations are highly restricted compared with that of **1c**.

(38) Mohamadi, F.; Richards, N. G. J.; Guida, W. C.; Liskamp, R.; Lipton, M.; Gaufield, C.; Chang, G.; Hendrickson, T.; Still, W. C. *J. Comput. Chem.* **1990**, *11*, 440.

(39) (a) Rehm, D.; Weller, A. *Isr. J. Chem.* **1970**, *7*, 259. (b) Mataga, N.; Miyasaka, H. In *Electron Transfer*; Jortner, J., Bixon, M., Eds.; John Wiley & Sons: New York, 1999; Part 2, pp 431−496.

(40) Kreher, D.; Hudhomme, P.; Gorgues, A.; Luo, H.; Araki, Y.; Ito, O. *Phys. Chem. Chem. Phys.* **2003**, *5*, 4583.

(41) (a) Arbogast, J. W.; Foote, C. S.; Kao, M. *J. Am. Chem. Soc.* **1992**, *114*, 2277−2279. (b) Biczok, L.; Linschitz, H. *Chem. Phys. Lett.* **1992**, *195*, 339−346. (c) Nonell, S.; Arbogast, J. W.; Foote, C. S. *J. Phys. Chem.* **1992**, *96*, 4169−4170. (d) Steren, C. A.; von Willigen, H.; Biczok, L.; Gupta, N.; Linschitz, H. *J. Phys. Chem.* **1996**, *100*, 8920. (e) Luo, C.; Fujitsuka, M.; Watanabe, A.; Ito, O.; Gan, L.; Huang, Y.; Huang, C.-H. *J. Chem. Soc., Faraday Trans.* **1998**, *94*, 527.

(42) (a) Fuhrhop, J.-H.; Mauzerall, D. J. *J. Am. Chem. Soc.* **1969**, *91*, 4147. (b) Chorsrowjan, H.; Taniguchi, S.; Okada, T.; Takagi, S.; Arai, T.; Tokumaru, K. *Chem. Phys. Lett.* **1995**, *242*, 644.

(43) (a) Marcus, R. A. *J. Chem. Phys.* **1956**, *24*, 966. (b) Marcus, R. A. *J. Chem. Phys.* **1965**, *43*, 679. (c) Marcus, R. A.; Sutin, N. *Biochim. Biophys. Acta* **1985**, *811*, 265.

(44) Yamazaki, M.; Araki, Y.; Fujitsuka, M.; Ito, O. *J. Phys. Chem. A* **2001**, *105*, 8615.

(45) (a) Watanabe, A.; Ito, O.; Watanabe, M.; Saito, H.; Koishi, M. *Chem. Commun.* **1996**, 117. (b) Fujitsuka, M.; Watanabe, A.; Ito O. *J. Phys. Chem. A* **1997**, *101*, 7960.

(46) (a) Yamanaka, K.; Fujitsuka, M.; Araki, Y.; Ito, O.; Aoshima, T.: Fukushima, T.; Miyashi, T. *J. Phys. Chem. A* **2004**, *108*, 250. (b) Makinoshima, T.; Fujitsuka, M.; Sasaki, M.; Araki, Y.; Ito, O.; Ito, S.; Morita, N. *J. Phys. Chem. A* **2004**, *108*, 368. (c) Nishikawa, H.; Kojima, S.; Kodama, T.; Ikemoto, I.; Suzuki, S.; Kikuchi, K.; Fujitsuka, M.; Luo, H.; Araki, Y.; Ito, O. *J. Phys. Chem. A* **2004**, *108*, 1881.